Clinical Neurophysiology 130 (2019) 1151–1159

Contents lists available at ScienceDirect

Clinical Neurophysiology

journal homepage: www.elsevier.com/locate/clinph

Hippocampal high frequency oscillations in unilateral and bilateral mesial temporal lobe epilepsy

Pavel Řehulka [a,*], Jan Cimbálník [b], Martin Pail [a], Jan Chrastina [c], Markéta Hermanová [d], Milan Brázdil [a,e]

[a] Brno Epilepsy Center, Department of Neurology, St. Anne's University Hospital and Faculty of Medicine, Masaryk University, Brno, Czech Republic
[b] International Clinical Research Center, St. Anne's University Hospital, Brno, Czech Republic
[c] Brno Epilepsy Center, Department of Neurosurgery, St. Anne's University Hospital and Faculty of Medicine, Masaryk University, Brno, Czech Republic
[d] Brno Epilepsy Center, First Department of Pathology, St. Anne's University Hospital and Faculty of Medicine, Masaryk University, Brno, Czech Republic
[e] Behavioral and Social Neuroscience Research Group, CEITEC – Central European Institute of Technology, Masaryk University, Brno, Czech Republic

ARTICLE INFO

Article history:
Accepted 13 March 2019
Available online 10 April 2019

Keywords:
High frequency oscillations
Hippocampus
Hippocampal sclerosis
Temporal lobe epilepsy
Bitemporal epilepsy

HIGHLIGHTS

- Hippocampal recordings in patients with mesial temporal lobe epilepsy were analyzed.
- Non-epileptic hippocampi demonstrated lower ripple rates than those epileptic.
- The highest fast ripple rate was seen in ventral parts of sclerotic hippocampi.

ABSTRACT

Objective: The main aim of this study was to investigate the potential differences in terms of interictal high frequency oscillations (HFOs) between both hippocampi in unilateral (U-MTLE) and bilateral mesial temporal lobe epilepsy (B-MTLE).
Methods: Sixteen patients with MTLE underwent bilateral hippocampal depth electrode implantation as part of epilepsy surgery evaluation. Interictal HFOs were detected automatically. The analyses entail comparisons of the rates and spatial distributions of ripples and fast ripples (FR) in hippocampi and amygdalae, with respect to the eventual finding of hippocampal sclerosis (HS).
Results: In U-MTLE, higher ripple and FR rates were found in the hippocampi ipsilateral to the seizure onset than in the contralateral hippocampi. Non-epileptic hippocampi in U-MTLE were distinguished by significantly lower ripple rate than in the remaining analyzed hippocampi. There were not differences between the hippocampi in B-MTLE. In the hippocampi with proven HS, higher FR rates were observed in the ventral than in the dorsal parts.
Conclusions: Non-epileptic hippocampi in U-MTLE demonstrated significantly lower ripple rates than those epileptic in U-MTLE and B-MTLE.
Significance: Low interictal HFO occurrence might be considered as a marker of the non-epileptic hippocampi in MTLE.

1. Introduction

Interictal high frequency oscillations (HFOs), ripples (80–250 Hz), and fast ripples (FRs; 250–600 Hz) have been studied over the past two decades and have been detected in different brain areas under physiological and pathological conditions. As the visual review of HFOs has several disadvantages (Gardner et al., 2007; Zelmann et al., 2009), interest has been dedicated to resolving problematic issues related to automated HFO detection (Birot et al., 2013; Navarrete et al., 2016; Waldman et al., 2018; Zelmann et al., 2012). Increase of FRs have been repeatedly demonstrated in the seizure onset zone and is thought to be a biomarker of epileptogenicity. In mesial temporal areas, ripples are associated mainly with the physiological functions of mesial temporal structures (Jacobs et al., 2008; Staba et al., 2002; Worrell et al., 2008). In the recordings from microelectrodes higher FR to ripple ratio were demonstrated in mesial temporal area ipsilateral to seizure onset than those contralateral (Staba et al., 2002, 2007). Moreover, the characteristic features of hippocampal sclerosis (hippocampal

* Corresponding author at: Department of Neurology, St. Anne's University Hospital and Faculty of Medicine, Pekařská 53, 656 91 Brno, Czech Republic. Fax: +420 543 182 624.
E-mail address: pavel.rehulka@fnusa.cz (P. Řehulka).

https://doi.org/10.1016/j.clinph.2019.03.026
1388-2457/

neuronal loss, reduced hippocampal volume) were found to be associated with greater FRs occurrence (Jacobs et al., 2009; Ogren et al., 2009; Staba et al., 2007).

Bitemporal epilepsy is characterized by independent seizure origins in both temporal lobes (Hirsch et al., 1991). The identification of bitemporal epilepsy requires invasive EEG recordings from both temporal lobes and should be considered as a dynamic, nonstationary condition due to possibility of the seizure clustering effect (Spencer et al., 2011) and long term seizure laterality switch (Smart et al., 2013). Consequently, it remains unclear whether bitemporal epilepsy represents a specific type of a single extensive epileptogenic network or two independent networks.

Several HFO studies have involved patients with bilateral mesial temporal seizure onset (Jacobs et al., 2008, 2009, 2010; Staba et al., 2002; Worrell et al., 2008), particularly when the investigated patients did not have a visible MRI lesion (Andrade-Valença et al., 2012). The involvement of patients with bitemporal epilepsy in such studies presumes the parity of both seizure onset zones and their equivalence with a seizure onset zone in unilateral temporal lobe epilepsy. This premise might carry a potential risk of selection bias. On the other hand, HFO analysis could reveal new insight into the pathophysiology of bitemporal epilepsy and provide useful information for the clinicians.

This retrospective study was conducted as a group comparison of the interictal HFOs occurrence in hippocampi ipsilateral and contralateral to the side of the seizure onset zone in mesial temporal lobe epilepsy. We hypothesize that in unilateral mesial temporal lobe epilepsy (U-MTLE) interictal HFO occurence is higher in epileptic than in non-epileptic hippocampi. In bilateral mesial temporal lobe epilepsy (B-MTLE) we aimed at both epileptic hippocampi (on the side with the higher and lower number of registered seizures) in order to establish potential differences between them. As the neuronal loss vary along the longitudinal axis of sclerotic hippocampi (Thom et al., 2012), the analyses were performed with respect to the underlying hippocampal pathology and recording site localization.

2. Methods

2.1. Patient selection

We reviewed all patients with intractable epilepsy who had undergone invasive EEG at a sampling rate of 5000 Hz at the Brno Epilepsy Center at St. Anne's University Hospital in Brno between January 2011 and March 2017. The study included the patients who fulfilled the following criteria: (1) seizure semiology compatible with mesial temporal lobe epilepsy (MTLE); (2) available recordings from depth electrodes implanted in both hippocampi; and (3) fitting in one of the two following groups:

1. Patients with U-MTLE who fulfilled criteria a and b:
   (a) All spontaneous seizures originated in the mesial structures of one temporal lobe;
   (b) At least one of the following three characteristics:
      (i) $\geq$ 5 recorded clinical seizures (implying acceptable confidence of only unilateral seizure onset zone (Blum, 1994)),
      (ii) 3 clinical and $\geq$3 subclinical (asymptomatic) seizures recorded (subclinical seizures are usually generated from the same temporal lobe as clinical seizures and predict favorable post-surgical outcomes (Sperling and O'Connor, 1990)),
      (iii) Engel IA classification for at least two years of follow-up care after anteromedial temporal resection.
2. Patients with B-MTLE – defined as those having recorded at least one independent spontaneous clinical seizure onset arising from both mesial temporal structures.

All patients underwent high-resolution MRI scans at 1.5 Tesla (Siemens Magnetom Symphony scanner) or 3 Tesla (GE Discovery 750 scanner). All patients signed an informed consent form. The study was approved by St Anne's University Hospital Research Ethics Committee and the Ethics Committee of Masaryk University.

2.2. Group and subgroup matching

In each patient with U-MTLE, the hippocampus on the side of all registered seizures was labelled as 'ipsilateral' (UNIP) and the other side as 'contralateral' (UNCO). Similarly, in each patient with B-MTLE, the hippocampus on the side with the higher number of registered seizures was labelled as 'ipsilateral' (BIP) and the other as 'contralateral' (BICO); in cases of parity of recorded seizures, the side of subsequent surgical intervention was labelled as 'ipsilateral'. In order to estimate the potential influence of underlying pathology on interictal HFOs occurrence, the following two groups of hippocampi with adjacent amygdalae were formed.

HS^+ group – hippocampus with evidence of hippocampal sclerosis (HS) based on MRI (clear hippocampal atrophy and an unequivocally increased signal from the hippocampus) and/or histopathological finding of HS as defined by the ILAE classification system (Blümcke et al., 2013).

HS^- group – hippocampus with histopathological finding of 'no-HS/gliosis only' as defined by ILAE classification (Blümcke et al., 2013).

2.3. Recording methods

All patients underwent video-EEG monitoring with multicontact depth electrodes inserted orthogonally into different parts of the brain including both hippocampi. In all patients were used 5-, 10-, or 15-contact platinum semiflexible Microdeep intracerebral electrodes (Alcis, France) with an electrode diameter of 0.8 mm, a contact length of 2 mm, with 3.5 mm center-to-center spacing (1.5 mm between contacts) and a surface area of 5 mm^2 for each contact. The anatomical targeting of intracerebral electrodes was individualized in each patient according to available non-invasive data and hypotheses about the seizure onset zone location. Interictal EEG recordings were low-pass filtered at 1000 Hz at a sampling rate of 5000 Hz (a reference average montage was used). A recording session in a noiseless Faraday room was performed prior to initiating the reduction of antiepileptic drugs (usually during the second post-implant day between 8 a.m. and 12 noon), in a wakeful resting state. The session duration differed among patients depending on individual collaboration capacity and patient comfort. Thirty minutes of interictal EEG activity were selected, having no or minimal artifacts, recorded at least 2 hours after and before a seizure.

2.4. Recording sites

Only contacts verified as located in the hippocampus (Hip) or amygdala (Amy) were used for HFO analysis. Hippocampal contacts were further subdivided into those placed in the head of the hippocampus (aHip) and those in the body or tail of the hippocampus (pHip). The localization of all implanted electrodes and contacts was determined visually by two independent experienced researchers (P.R. and M.P.). Post-implant 1.5-Tesla MRI study (T2-weighted Turbo Inversion Recovery Magnitude sequence in axial, coronal, and sagittal planes) with depth electrodes in situ

was used. The location of each electrode and contact was ultimately determined using the MRI atlas by Tamraz and Comair (2000). The anatomical boundaries of the hippocampus were based on a reference atlas (Duvernoy et al., 2013).

2.5. Histopathological examination

Histopathological examinations were performed only for those patients who had undergone resective surgery. "All the paraffin-embedded tissue specimens, slides, and histopathology reports were retrieved from the files of the First Department of Pathology of St. Anne's University Hospital. All examined resected tissues were identically treated, fixed in a 10% neutral buffered formalin, grossly inspected, carefully oriented, measured, and cut so as to obtain representative 2–3 mm thick tissue slices perpendicular to the cortical surface. Smaller resection specimens were completely processed and paraffin embedded; in larger resection specimens, at least every second tissue slice was further processed. Five micrometer thick tissue sections were stained by hematoxylin and eosin (H&E), and evaluated under light microscope. NeuN immunohistochemistry (using mouse monoclonal anti-NeuN antibody, dilution 1:100, clone A-60, Millipore) was performed on preselected tissue sections if there was an inconclusive picture in H&E" (Kuba et al., 2013). The classification system for HS proposed by the ILAE (Blümcke et al., 2013) was applied.

2.6. Automated detection of HFOs

HFOs were detected by a custom-made Python detection algorithm (Kucewicz et al. 2014). The signal in the statistical window (10 s) was filtered in a series of 400 logarithmically spaced frequency bands ranging from 30–800 Hz. Power envelopes and their corresponding z-scores were computed for each band. Putative detections were obtained as events >3.5 of the z-score. Putative detections in adjacent frequency bands and overlaps in the temporal domain were joined and considered a single event. Event onsets and offset were determined as the first and last values above the threshold in all the frequency bands of the putative detections. The highest z-score values of the putative detections were used to obtain event frequencies. The detections were separated into ripples (80–250 Hz) and FRs (250–600 Hz). Events with frequencies below 80 Hz and above 600 Hz were disregarded as well as events shorter than 4 oscillations at the peak frequency. This led to the successful elimination of filter artifacts produced by sharp transients since the highest z-score values of such events are in low frequencies and their estimated frequency is below 80 Hz. The procedure is illustrated in Supplementary Fig. 1. Ripple and FR incidence was expressed as the rate of respective events per 10 minutes (No./10 min).

Detector validation was done in a similar fashion as in a study by Roehri et al. (2016). Simulated HFOs, HFOs on spike, and spikes were inserted into a signal recorded from non-pathological white matter. The parameters of each inserted HFO event were pseudo-randomized with varying frequency (80–600 Hz), duration (6–10 oscillations at the given frequency), and amplitude (0.05–0.25 of signal std). The HFOs were constructed as tapering sine waves. Similarly, the parameters of inserted spikes were varied for duration (0.05–0.2 s) and amplitude (2.5–12.5 of signal std). Events were inserted in 3 s time windows and algorithm precision-recall was calculated. The resulting performance was 0.94 precision and 0.72 recall.

2.7. Statistical analysis

Custom Python scripts were created for statistical analyses using the SciPy module. The data were tested for normal distribution using D'Agostino's normality test. Since most of the data sets failed this test, the Wilcoxon rank sum test was used to evaluate differences among them. Bonferroni's correction was applied where necessary.

To evaluate whether normal hippocampal tissue (UNCO) can be distinguished from pathological hippocampal tissue (UNIP, BIP, BICO), receiver operating characteristic (ROC) curves and their area under the curve (AUC) were calculated on per channel basis using HFO rates as the varying threshold. This analysis was performed on a per hippocampus basis and separately for aHip and pHip. The statistical significance of AUCs compared to chance (AUC = 0.5) was tested with Hanley-McNeil test.

3. Results

3.1. Description of study population and recording sites data set

Of the 62 consecutive patients recorded at a sampling rate of 5000 Hz, 16 patients met the inclusion criteria for the study: 9 patients with U-MTLE and 7 patients with B-MTLE. Individual characteristics of all patients are summarized in Table 1 and a comparison of clinical variables between both groups is provided in Table 2. Notably, in patients 7 and 14 temporopolar seizures that arose concurrently from the temporal pole and the hippocampus were observed. Interictal recordings were available from the both hippocampal sides in patients with U-MTLE (9 UNIP and 9 UNCO) or with B-MTLE (7 BIP and 7 BICO). The HS^{+} group comprised 6 UNIP and 1 BIP, the HS^{-} group had two pairs of UNIP and BIP. The localization of recording sites and contacts among these groups is indicated in Table 3.

3.2. Hippocampal HFOs in U-MTLE

First, to establish the potential difference between hippocampi ipsilateral and contralateral to seizure onset zone in U-MTLE, we compared homotopic recording sites in UNIP and UNCO. Higher rates were observed in UNIP than in UNCO, in both aHip (ripples: 126.17 ± 102.93 and 31.83 ± 27.32 [$p < 0.001$], FRs: 160.17 ± 162.68 and 32.13 ± 24.67 [$p = 0.003$], respectively) and pHip (ripples: 134.15 ± 101.37 and 18.25 ± 21.60 [$p \ll 0.001$], FRs: 71.30 ± 69.44 and 17.13 ± 17.17 [$p = 0.003$], respectively) recording sites. The results are illustrated in Fig. 1. In order to test whether difference between UNIP and UNCO might be attributed to the difference between epileptic and non-epileptic hippocampal tissue we proceeded with ROC analysis between the hippocampi contralateral (UNCO) and ipsilateral (UNIP, BIP, BICO) to seizure onset. Hanley-McNeil test reached statistical significance in the ripple range both in aHip (AUC = 0.734, $p = 0.014$) and pHip (AUC = 0.788, $p = 0.002$), indicating that a low hippocampal ripple rate might be sufficient to identify hippocampus without obvious involvement in seizure onset (Fig. 2). A similar but non-significant trend was found in the FR range within aHip (AUC = 0.668, $p = 0.057$).

3.3. Hippocampal HFOs in B-MTLE

Similarly were compared homotopic recording sites in B-MTLE. BIP and BICO did not differ significantly, in either aHip (ripples: 90.62 ± 47.82 and 80.41 ± 78.29, FRs: 54.29 ± 34.52 and 70.22 ± 71.68, respectively) or pHip (ripples: 60.61 ± 38.79 and 37.86 ± 42.89, FRs: 26.78 ± 32.18 and 22.04 ± 24.32, respectively) recording sites (Fig. 1).

Table 1
Individual characteristics of patients in the U-MTLE and B-MTLE groups.

No./ Group	Sex/ Age	Duration (years)/PF	MRI finding/ scanner	PET hypo-metabolism	Explored brain lobes (No. of electrodes)	Side, No. and SOZ of seizures #	AMTR*	Histopathology**	VNS***	Previous intervention/**
1/U	F/56	28/-	R/HA/1.5T	R/mT	T (2), T′(3)	R: 5 mT [R]	R/IIIA (5)	NA	NP	NP
2/U	F/33	31/ME	L/HS, PECLT/3T	L/mT	T(2), T′(6), F′(3)	L: 3 mT	L/IA (3)	HS type 1	NP	NP
3/U	F/27	18/ME	L/HS/3T	L/Tp	T′(8), T(2), P′(1), I′(1), F′(1)	L: 3 mT [L]	L/IIIA (3)	HS type 1, FCD IIIa	NP	NP
4/U	M/51	49/FS	R/HA /3T	R/mT	T(5), F(3), T′(2)	R: 3 mT [R]	R/IA (3)	HS type 2	NP	NP
5/U	M/24	14/TBI	L/HS, MPTG/3T	L/mT, P	T(2), T′(7)	L: 3 mT [L]	L/IIA(2)	pHS	NP	NP
6/U	F/45	19/-	L/HA/3T	normal	T(2), T′(8), I′(1), P′(1), F′(2)	L: 3 mT [L]	L/IIIA (2)	no-HS	NP	NP
7/U	F/36	27/-	R,L/HIMAL/3T	normal	T(7), T′(3)	R: 2 Tp, 1 mT	R/IA (2)	no-HS	NP	NP
8/U	F/26	20/-	R/HS/3T	R/mT	T(4), T′(2), F (4), I(1), P (1)	R: 6 mT	R/IA (1)	HS type 1	NP	NP
9/U	F/56	55/ME	R/HS/3T	R/mT	T(5), F(2),T′(4)	R: 7 mT	R/IVA (1)	HS type 2	NP	VNS
10/B	F/20	4/-	normal/1.5T	L/Tp	T (3), T′(2) §	R: 10 mT; L: 1 mT	NP	NA	IIIB (5)	LTPR†/normal
11/B	F/34	30/-	R/HA/1.5T	R/mT	T′(3), T(3)	R: 3 mT; L: 1 mT [R > L]	R/IA (5)	pHS	NP	NP
12/B	F/33	17/PI	normal/1.5T	R,L/mT	T′(4), T(4)	R: 4 mT; L: 1 mT	R/IIIA (5)	no-HS	NP	VNS
13/B	M/38	11/-	normal/3T	L/Tp	T(3), I′(2), T′(6), P′(1), O′(1), F′(1)	R: 4 mT; L: 1 mT	NP	NA	IIB (4)	NP
14/B	M/35	14/-	R,L/HA/3T	R > L mT	T(6), T′(2)	R: 4 Tp; L: 1 mT [L]	NP	NA	IIIB (2)	NP
15/B	M/37	6/FS	normal/3T	L/mT, Tp	T′(8), F′(2), T(2)	L: 2 mT; R: 2 mT	L/IA (3)	no-HS	NP	NP
16/B	F/58	46/-	L/HS/1.5T	NA	T (1), T′(2), F′(3)	R: 2 mT; L: 5 mT [L]	NP	pHS	NP	LAMTR††/pHS

U – unilateral MTLE, B – bilateral MTLE; F – female; M – male; PF – precipitating factor; ME – meningoencephalitis; FS – febrile seizures; TBI – traumatic brain injury; PI – perinatal insult; MRI – magnetic resonance imaging; PET – positron emission tomography with ^{18}F – fluorodeoxyglucose; R – right; L – left; HS – hippocampal sclerosis; HA – hippocampal atrophy; PECLT – postencephalic changes of left temporal lobe; MPTG – mild posttraumatic gliosis of left pericentral region; HIMAL – hippocampal malrotation; mT – mesial temporal region; Tp – temporal pole; NA – not available; T – right temporal; T′ – left temporal; F – right frontal; F′ – left frontal; P – right parietal; P′ – left parietal; I – right insular; I′ – left insular; O′ – left occipital; § – recordings from one oblique electrode inserted into the body and tail of the left hippocampus were not analysed; SOZ – seizure onset zone; # – only clinical spontaneous seizures are indicated, the lateralization of electrophysiological seizures is mentioned in square brackets, if applicable; AMTR – anteromedial temporal lobe resection; * – side of AMTR/outcome using Engel classification (follow-up in years); NP – not performed; ** – histopathological finding using ILAE 2013 classification for hippocampal sclerosis, ILAE 2011 classification for focal cortical dysplasia; FCD – focal cortical dysplasia; pHS – probable hippocampal sclerosis as defined by ILAE 2013 classification for hippocampal sclerosis; VNS – vagus nerve stimulation; *** – outcome using McHugh classification (follow-up in years); LTPR – left temporal pole resection, † – based on non-invasive findings and data acquired during previous invasive EEG using unilateral covering only; L – left AMTR; †† – only the anterior portion of the hippocampus with a length of 15 mm was removed.

Table 2
Comparison of clinical characteristics between U-MTLE and B-MTLE group (median is calculated; range is given in square brackets).

	U-MTLE	B-MTLE	p-value
Number of patients	9	7	
Females	7	4	NS*
Age at evaluation (years)	36 [26–56]	35 [20–58]	NS**
Epilepsy duration (years)	27 [18–55]	14 [4–46]	p = 0.04**
Seizure frequency (per month)	4 [1–20]	6 [1–15]	NS**

NS – non significant; * – Fisher's exact test; ** – Mann-Whitney test.

3.4. Differences along the longitudinal hippocampal axis in U-MTLE and B-MTLE

In order to elaborate the issue of the potential influence of recording site location, we compared HFO rates between ventral (aHip) and dorsal (pHip) hippocampal recording sites in U-MTLE and B-MTLE. Higher FR rates were found in aHip than in pHip in UNIP (160.17 ± 162.68 and 71.30 ± 69.44, respectively; $p = 0.038$) and BIP (54.29 ± 34.52 and 26.78 ± 32.18, respectively; $p = 0.027$); statistically significant differences were nearly reached in BICO (70.22 ± 71.68 and 22.04 ± 24.32, respectively; $p = 0.051$) and UNCO (32.13 ± 24.67 and 17.13 ± 17.17, respectively; $p = 0.057$). Conversely, in the ripple range no statistically significant differences were observed between aHip and pHip in any studied group (UNIP: 126.17 ± 102.93 and 134.15 ± 101.37; BIP: 90.62 ± 47.82 and 60.61 ± 38.79; UNCO: 31.83 ± 27.32 and 18.25 ± 21.60; BICO: 80.41 ± 78.29 and 37.86 ± 42.89, respectively).

3.5. Hippocampal HFOs in HS$^+$ and HS$^-$ subgroups

To estimate the potential influence of underlying hippocampal pathology, we compared homotopic recording sites in the HS$^+$ and HS$^-$ subgroups (Fig. 3). In aHip, higher ripple (141.72 ± 95.93, 70.46 ± 44.26; $p = 0.017$) and FR rates (173.59 ± 163.15, 54.54 ± 38.3; $p = 0.015$) were observed in the former subgroup than in the latter; in pHip, the higher rate was statistically significant only in the ripple range (151.45 ± 101.54, 49.43 ± 34.21; $p = 0.001$). In amygdalar recording sites, higher ripple rates were found in the HS$^+$ group (85.0 ± 52.13) than the HS$^-$ group (34.10 ± 20.78; $p = 0.006$); a similar trend in the FR band was statistically non-significant (61.18 ± 60.69 and 22.60 ± 15.57; $p = 0.06$).

3.6. Differences along the longitudinal hippocampal axis in HS$^+$ and HS$^-$ subgroups

Finally, potential differences in terms of HFO rates along the longitudinal axis of the amygdalo-hippocampal complex were examined. In the HS$^+$ subgroup, a higher ripple rate was found in pHip (151.45 ± 101.54) than in Amy (85.0 ± 52.13; $p = 0.03$); the difference between aHip and Amy nearly reached statistical significance (141.72 ± 95.93 and 85.0 ± 52.13, respectively; $p = 0.057$). In the FR band, the rate in aHip (173.59 ± 163.15) prevailed over those in both Amy (61.18 ± 60.69; $p = 0.013$) and pHip (71.25 ± 75.50; $p = 0.043$) (Fig. 4). In the HS$^-$ group, there were no significant differences among Amy, aHip, and pHip recording sites in the ripple range or in the FR range.

4. Discussion

4.1. Hippocampal HFOs and unilateral MTLE

Majority of the fundamental HFO literature is based upon the comparison of the seizure onset zone versus non-seizure zone HFO occurence, regardless the anatomical boundaries of the

Table 3
The location of analyzed contacts in different recording sites (the number of recording contacts in brackets) among the respective groups (UNIP, UNCO, BIP, BICO – as defined in Section 2.2).

Patient no.	UNIP	UNCO	BIP	BICO
1	R: Amy (2), aHip (4)	L: Amy (3), aHip (3), pHip (4)	NA	NA
2	L*: Amy (3), aHip (3), pHip (3)	R: aHip (4), pHip (3)	NA	NA
3	L*: Amy (4), aHip (3), pHip (4)	R: aHip (3), pHip (3)	NA	NA
4	R*: Amy (2), aHip (3), pHip (2)	L: aHip (3), pHip (4)	NA	NA
5	L*: Amy (3), aHip (3), pHip (2)	R: aHip (2), pHip (2)	NA	NA
6	L**: Amy (3), aHip (3), pHip (3)	R: aHip (3), pHip (3)	NA	NA
7	R**: Amy (3), aHip (3), pHip (3)	L: Amy (3), aHip (2), pHip (3)	NA	NA
8	R*: Amy (3), aHip (3), pHip (3)	L: aHip (2), pHip (2)	NA	NA
9	R*: Amy (4), aHip (3), pHip (3)	L: Amy (4), aHip (2), pHip (1)	NA	NA
10	NA	NA	R: Amy (4), aHip (3), pHip (3)	L: aHip (4)
11	NA	NA	R*: Amy (3), aHip (4), pHip (3)	L: Amy (3), aHip (4), pHip (3)
12	NA	NA	R**: Amy (4), aHip (3), pHip (4)	L: Amy (2), aHip (4), pHip (3)
13	NA	NA	R: Amy (3), aHip (3), pHip (3)	L: Amy (4), aHip (7), pHip (2)
14	NA	NA	R: Amy (3), aHip (4), pHip (3)	L: aHip (2), pHip (3)
15	NA	NA	L**: aHip (4), pHip (4)	R: Amy (3), aHip (3)
16	NA	NA	L: pHip (3)	R: aHip (2)
Amy contacts	27	10	17	12
aHip contacts	28	24	21	26
pHip contacts	23	25	23	11

R – right; L – left; Amy – amygdala; aHip – anterior hippocampus; pHip – posterior hippocampus; NA – not applicable; * – HS^{+} subgroup as defined in Section 2.2; ** – HS^{-} group subgroup as defined in Section 2.2. The sum of contacts for the respective groups in different recording sites is provided at the bottom of the table.

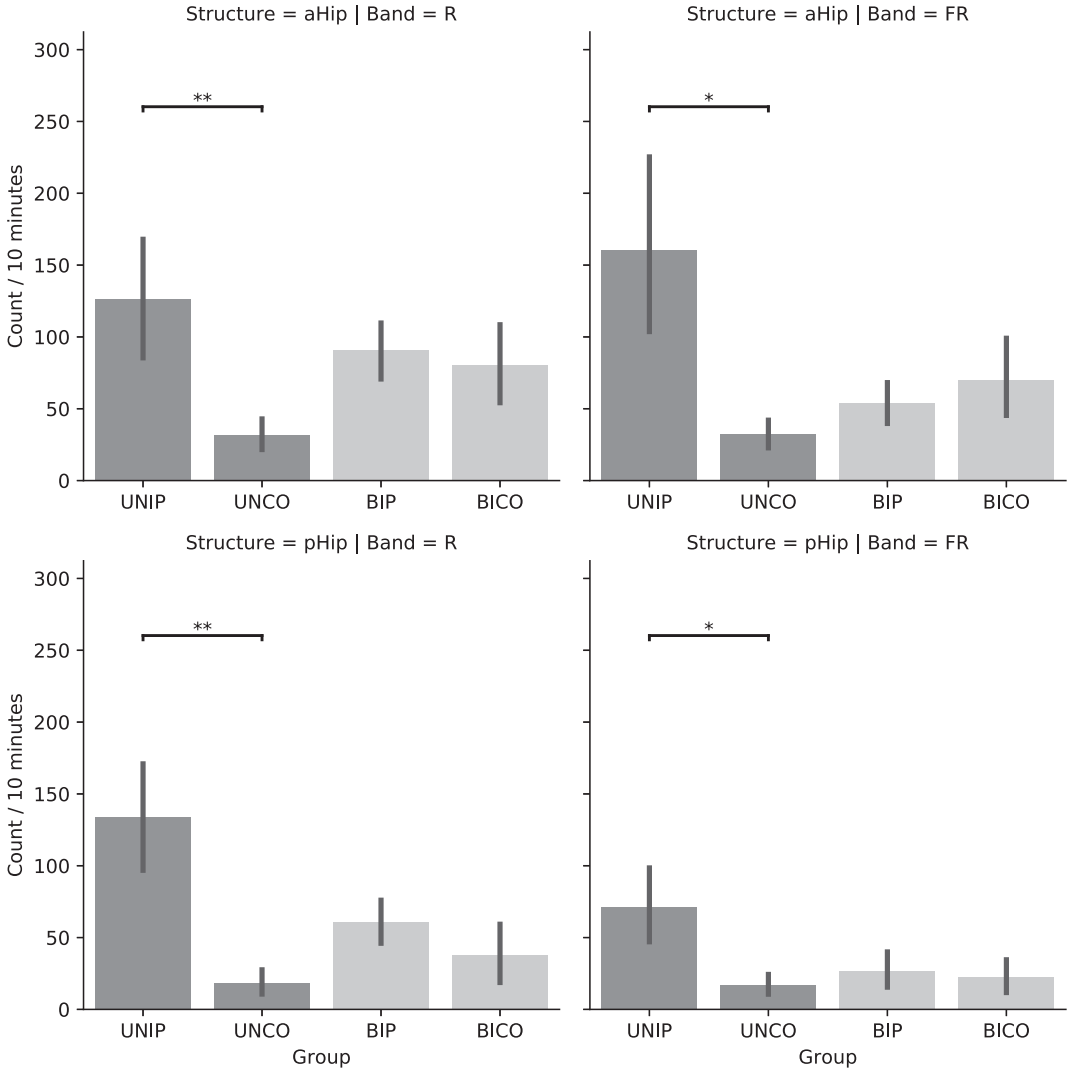

Fig. 1. Differences between ipsilateral and contralateral hippocampi in patients with unilateral (UNIP and UNCO, respectively) and bilateral (BIP and BICO, respectively) mesial temporal lobe epilepsy. The analysis was performed separately for ventral (aHip) and dorsal (pHip) hippocampal recording sites in ripple (R) and fast ripple (FR) bands. Significance levels are marked by asterisks (* < 0.05, ** < 0.001).

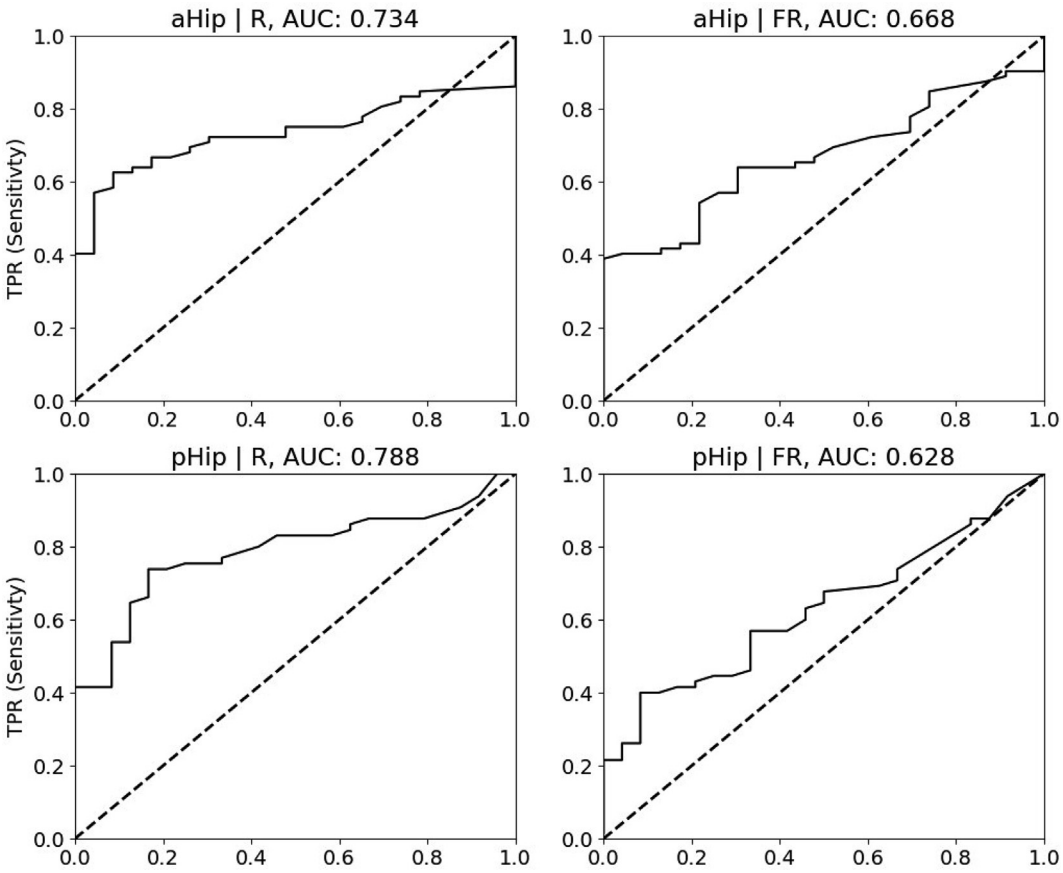

Fig. 2. The receiver operating characteristics (ROC) curves were created by plotting the true positive rates (TPR) against the false positive rates (FPR) in order to evaluate whether the hippocampi contralateral (UNCO) and ipsilateral to seizure onset (UNIP, BIP, BICO groups) can be distinguished. Each area under the curve (AUC) was compared to chance (AUC = 0.5 represented by the dashed line) and tested with Hanley-McNeil test. The statistical significance (p-value <0.05) was reached both for the anterior (aHip; AUC = 0.734) and posterior hippocampus (pHip; AUC = 0.788) in ripple (R), but not in fast ripple (FR) range.

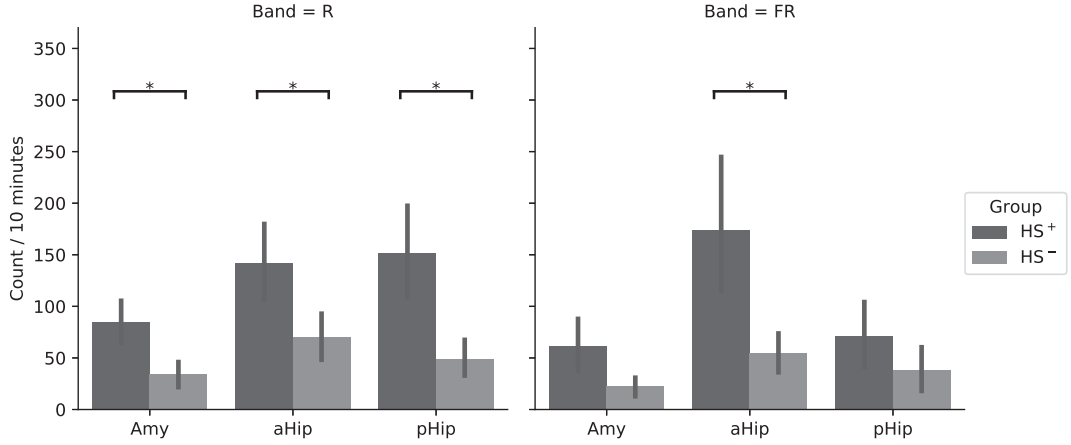

Fig. 3. Comparison of ripple (R) and fast ripple (FR) rates in homotopic recording sites (Amy – amygdala, aHip – anterior hippocampus, pHip – posterior hippocampus) with respect to the underlying pathology (HS^+ subgroup – hippocampal sclerosis, HS^- subgroup – no– hippocampal sclerosis /gliosis only). The significance level <0.05 is indicated by asterisks (*). Please note the higher R rates in either Amy, aHip and pHip recording sites in HS^+ than in HS^- subgroup. The similar trend in the FR range reached statistical significance only in the ventral parts of sclerotic hippocampi.

explored structures or mesial temporal and lateral neocortical localization. Indeed, ripple and FR rates that were found higher in the seizure onset zone than outside if clinical macroelectrodes were used (Jacobs et al., 2008; Jacobs et al., 2009; Andrade-Valença et al., 2012). In studies dedicated to the comparison between mesial temporal areas ipsilateral and contralateral seizure onset zones (recordings from microelectrodes) showed higher FR to ripple ratio in ipsilateral mesial area (Staba et al., 2002, 2007).

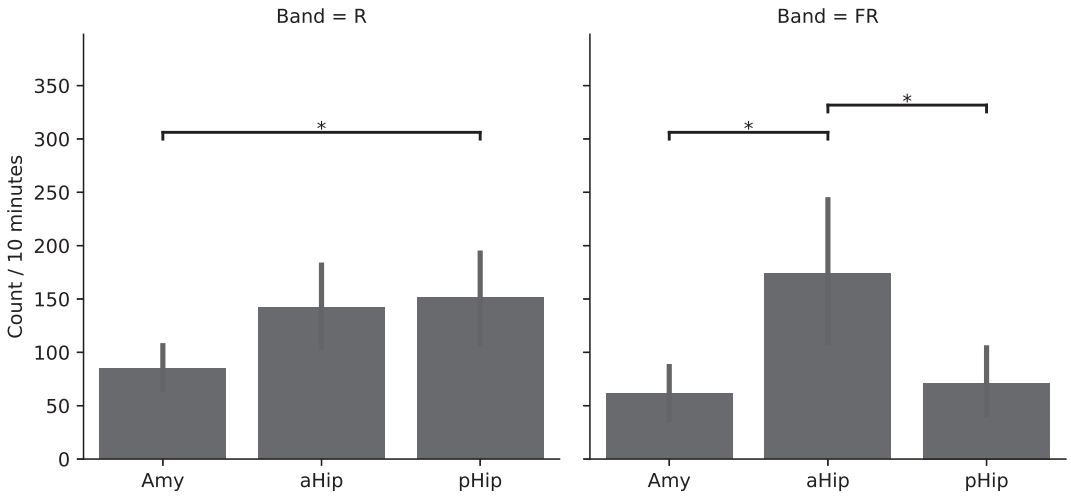

Fig. 4. Ripple (R) and fast ripple (FR) rates in recording sites along the longitudinal axis of the amygdalo-hippocampal complex in the HS^{+} subgroup (Amy – amygdala, aHip – anterior hippocampus, pHip – posterior hippocampus). The significance level of <0.05 is marked by asterisks (*). Please note the most increased FR rate in the ventral part of sclerotic hippocampi and the lacking difference between ventral and dorsal part of sclerotic hippocampi in the R band. Differences in the HS^{-} subgroup did not reach statistical significance (not illustrated).

In present study higher ripple and FR rates were found in the hippocampi ipsilateral to the seizure onset than in the contralateral hippocampi in U-MTLE. Moreover, non-epileptic hippocampi demonstrated significantly lower ripple rates than others. However, it remains questionable whether this finding might support the opinion that FR-generating areas are relatively stable (Bragin et al., 2003) as the recent study provided the detailed analysis indicating substantial spatiotemporal variability of HFOs (Gliske et al., 2018). It is doubtful whether the low interictal HFO rate might be used as a negative biomarker of the non-epileptic hippocampi. In any case, the challenging issue of HFO specificity should be resolved by prospective studies on a per subject basis.

4.2. Hippocampal HFOs and bilateral MTLE

In an experimental rat model of induced temporal lobe epilepsy, unilateral lesion in the hippocampus was sufficient for the later occurrence of independent bilateral seizures and interictal FRs within both hippocampi (Finnerty and Jefferys, 2002; Jefferys and Empson, 1990; Bragin et al., 2003; Jiruska et al., 2010). The literature presents limited evidence that the epileptogenic network in bilateral MTLE is more spatially extended, concerning the extrahippocampal mesial temporal structures, than that in unilateral MTLE (Aubert et al., 2016; Bragin et al., 2003; Jacobs et al., 2009). This might increase the number and variability of potential ictal generators among extrahippocampal structures; this has been demonstrated in unilateral MTLE (Spencer and Spencer, 1994; Van Paesschen et al., 2001; Wennberg et al., 2002). It might be interesting to clarify the role of the extrahippocampal structures within the epileptogenic network in bitemporal epilepsy.

Secondly, there is evidence for progressive cellular and network alterations in MTLE (Pitkänen and Sutula, 2002; Bartolomei et al., 2008). Some works have proposed a process of secondary epileptogenesis as a possible mechanism of bitemporal epilepsy development (Morrell, 1989; Wilder, 2001). Indeed, in an experimental rat model FRs within both hippocampi and bilateral spontaneous seizures developed during the first weeks after a unilateral intrahippocampal tetanus toxin injection (Finnerty and Jefferys, 2002; Jiruska et al., 2010). Nevertheless, this finding of a short-term process leading to bilateral disorder in rodents must be interpreted carefully when considering the different hippocampal commissural system arrangement in humans (Gloor et al., 1993). In the present study, patients with unilateral MTLE demonstrated significantly longer epilepsy duration than patients with bilateral MTLE, although previously no difference was observed between both groups (Hirsch et al., 1991). Unfortunately, in the present study, the small sample size did not allow the correlation between the HFO rates and epilepsy duration. We wonder if a prospective design could be applied in human studies.

4.3. Interictal HFOs in MTLE, underlying hippocampal pathology and recording site localization

The increased FR rate in mesial temporal structures was previously found to be associated with the characteristic features of HS, such as hippocampal neuronal loss (Staba et al., 2007) and reduced hippocampal volume (Jacobs et al., 2009; Ogren et al., 2009; Staba et al., 2007). Our results indicate that it is possible that neuronal loss in sclerotic hippocampi might cause additional increases in HFO rates also in the ripple range, as has been suggested in previous studies (Jacobs et al., 2009; Worrell et al., 2008). Our finding of higher FR rates in the head than in the posterior parts of sclerotic hippocampi might be explained by the similar gradient of atrophy and neuronal loss within the sclerosis along the longitudinal hippocampal axis, which has been observed in both MRI and histopathological studies (Babb et al., 1984; Bernasconi et al., 2003; Thom et al., 2012). Another question is whether the HFO rate in amygdalar recording sites might be affected by amygdalar sclerosis, which is often associated with HS (Yilmazer-Hanke et al., 2000). It seems necessary to confirm and estimate the potential influence of these variables on the occurrence of HFOs.

4.4. Study limitations

Our results might be influenced by the high inter-individual variability of interictal HFOs and the small sample size. As bitemporal epilepsy might be a cause of surgery failure, in two patients the recordings were acquired during the re-evaluation procedure after a previous intervention in the temporal lobe (both hippocampi of patient 10 were completely intact; only registrations from contacts located in the spared left pHip were available in patient 16). As we understand the potential influence of previous interventions on hippocampal epileptogenicity, the influence is thought to be linked to the nature of mesial temporal sclerosis

per se, rather than its maturation in a surgical scar (Hennessy et al., 2000).

Visual inspection of the hippocampus with 3-Tesla MRI is not considered sensitive enough to detect all cases of HS (Blümcke et al., 2013). It is not possible to definitively exclude the possibility of HS in any hippocampi not examined histopathologically. Another limitation of this work was caused by the lack of criteria and the variable terminology used in bitemporal epilepsy description. Our B-MTLE patients were definitely characterized by independent seizure onsets; in patients with U-MTLE, it was not possible to exclude certain levels of involvement of both temporal lobes (as might be suggested by, e.g., frequent findings of bilateral interictal discharges (Ergene et al., 2000)). We minimized the risk of contamination in U-MTLE patients using multiple inclusion criteria. We used the terms 'ipsilateral'/'contralateral' to label each side of the hippocampi in order to avoid similar terms (such as 'primary', 'leading'/'secondary', 'mirror') that might suggest a certain pathophysiological concept.

Ultimately, the question remains whether bitemporal epilepsy represents a specific type of a single extensive epileptogenic network, as supported by a favorable outcome after unilateral surgery (Aghakhani et al., 2014), or two independent networks, as is indirectly expressed in its definition. We encourage further research with the purpose of bringing together the two perspectives.

Conflict of interest

None of the authors has any conflict of interest to disclose.

Acknowledgments

This work was supported by funds from the Faculty of Medicine, Masaryk University, provided to the junior researcher (Martin Pail).

We confirm that we have read the journal's position on the issues involved in ethical publication and affirm that this report is consistent with those guidelines.

We thank Anne Johnson for grammatical assistance.

Appendix A. Supplementary material

Supplementary data to this article can be found online at https://doi.org/10.1016/j.clinph.2019.03.026.

References

Aghakhani Y, Liu X, Jette N, Wiebe S. Epilepsy surgery in patients with bilateral temporal lobe seizures: a systematic review. Epilepsia 2014;55:1892–901.
Andrade-Valença L, Mari F, Jacobs J, Zijlmans M, Olivier A, Gotman J, et al. Interictal high frequency oscillations (HFOs) in patients with focal epilepsy and normal MRI. Clin Neurophysiol 2012;123:100–5.
Aubert S, Bonini F, Curot J, Valton L, Szurhaj W, Derambure P, et al. The role of subhippocampal versus hippocampal regions in bitemporal lobe epilepsies. Clin Neurophysiol 2016;127:2992–9.
Babb TL, Lieb JP, Brown WJ, Pretorius J, Crandall PH. Distribution of pyramidal cell density and hyperexcitability in the epileptic human hippocampal formation. Epilepsia 1984;25:721–8.
Bartolomei F, Chauvel P, Wendling F. Epileptogenicity of brain structures in human temporal lobe epilepsy: a quantified study from intracerebral EEG. Brain 2008;131:1818–30.
Bernasconi N, Bernasconi A, Caramanos Z, Antel SB, Andermann F, Arnold DL. Mesial temporal damage in temporal lobe epilepsy: a volumetric MRI study of the hippocampus, amygdala and parahippocampal region. Brain 2003;126:462–9.
Birot G, Kachenoura A, Albera L, Bénar C, Wendling F. Automatic detection of fast ripples. J Neurosci Methods 2013;213:236–49.
Blum D. Prevalence of bilateral partial seizure foci and implications for electroencephalographic telemetry monitoring and epilepsy surgery. Electroencephalogr Clin Neurophysiol 1994;91:329–36.
Blümcke I, Thom M, Aronica E, Armstrong DD, Bartolomei F, Bernasconi A, et al. International consensus classification of hippocampal sclerosis in temporal lobe epilepsy: a Task Force report from the ILAE Commission on Diagnostic Methods. Epilepsia 2013;54:1315–29.
Bragin A, Wilson CL, Engel J. Spatial stability over time of brain areas generating fast ripples in the epileptic rat. Epilepsia 2003;44:1233–7.
Duvernoy HM, Cattin F, Risold PY. The Human Hippocampus: Functional Anatomy, Vascularization and Serial Sections with MRI. Berlin Heidelberg: Springer-Verlag; 2013.
Ergene E, Shih JJ, Blum DE, So NK. Frequency of bitemporal independent interictal epileptiform discharges in temporal lobe epilepsy. Epilepsia 2000;41:213–8.
Finnerty GT, Jefferys JGR. Investigation of the neuronal aggregate generating seizures in the rat tetanus toxin model of epilepsy. J Neurophysiol 2002;88:2919–27.
Gardner AB, Worrell GA, Marsh E, Dlugos D, Litt B. Human and automated detection of high-frequency oscillations in clinical intracranial EEG recordings. Clin Neurophysiol 2007;118:1134–43.
Gliske SV, Irwin ZT, Chestek C, Hegeman GL, Brinkmann B, Sagher O, Garton HJL, Worrell GA, Stacey WC. Variability in the location of high frequency oscillations during prolonged intracranial EEG recordings. Nat Commun 2018;9:2155.
Gloor P, Salanova V, Olivier A, Quesney LF. The human dorsal hippocampal commisure. An anatomically identifiable and functional pathway. Brain 1993;116:1249–73.
Hennessy MJ, Elwes RD, Binnie CD, Polkey CE. Failed surgery for epilepsy. A study of persistence and recurrence of seizures following temporal resection. Brain 2000;123:2445–66.
Hirsch LJ, Spencer SS, Williamson PD, Spencer DD, Mattson RH. Comparison of bitemporal and unitemporal epilepsy defined by depth electroencephalography. Ann Neurol 1991;30:340–6.
Jacobs J, LeVan P, Chander R, Hall J, Dubeau F, Gotman J. Interictal high-frequency oscillations (80–500 Hz) are an indicator of seizure onset areas independent of spikes in the human epileptic brain. Epilepsia 2008;49:1893–907.
Jacobs J, Levan P, Châtillon CE, Olivier A, Dubeau F, Gotman J. High frequency oscillations in intracranial EEGs mark epileptogenicity rather than lesion type. Brain 2009;132:1022–37.
Jacobs J, Zijlmans M, Zelmann R, Chatillon CE, Hall J, Olivier A, et al. High-frequency electroencephalographic oscillations correlate with outcome of epilepsy surgery. Ann Neurol 2010;67:209–20.
Jefferys JGR, Empson RM. Development of chronic secondary epileptic foci following intrahippocampal injection of tetanus toxin in the rat. Exp Physiol 1990;75:733–6.
Jiruska P, Finnerty GT, Powell AD, Lofti N, Cmejla R, Jefferys JG. Epileptic high-frequency network activity in a model of non-lesional temporal lobe epilepsy. Brain. 2010;133:1380–90.
Kuba R, Musilová K, Vojvodič N, Tyrlíková I, Rektor I, Brázdil M. Rhythmic ictal nonclonic hand (RINCH) motions in temporal lobe epilepsy: invasive EEG findings, incidence, and lateralizing value. Epilepsy Res 2013;106:386–95.
Kucewicz MT, Cimbalnik J, Matsumoto JY, Brinkmann BH, Bower MR, Vasoli V, et al. High frequency oscillations are associated with cognitive processing in human recognition memory. Brain 2014;137:2231–44.
Morrell F. Varieties of human secondary epileptogenesis. J Clin Neurophysiol 1989;6:227–75.
Navarrete M, Pyrzowski J, Corlier J, Valderrama M, Le Van Quyen M. Automated detection of high-frequency oscillations in electrophysiological signals: methodological advances. J Physiol Paris 2016;110:316–26.
Ogren JA, Wilson CL, Bragin A, Lin JJ, Salamon N, Dutton RA, et al. Three-dimensional surface maps link local atrophy and fast ripples in human epileptic hippocampus. Ann Neurol 2009;66:783–91.
Pitkänen A, Sutula TP. Is epilepsy a progressive disorder? Prospects for new therapeutic approaches in temporal-lobe epilepsy. Lancet Neurol 2002;1:173–81.
Roehri N, Lina JM, Mosher JC, Bartolomei F, Bénar CG. Time-frequency strategies for increasing high frequency oscillation detectability in intracerebral EEG. IEEE Trans Biomed Eng 2016;63:2595–606.
Smart O, Rolston JD, Epstein CM, Gross RE. Hippocampal seizure-onset laterality can change over long timescales: a same-patient observation over 500 days. Epilepsy Behav Case Rep 2013;1:56–61.
Spencer D, Gwinn R, Salinsky M, O'Malley JP. Laterality and temporal distribution of seizures in patients with bitemporal independent seizures during a trial of responsive neurostimulation. Epilepsy Res 2011;93:221–5.
Spencer SS, Spencer DD. Entorhinal-hippocampal interactions in medial temporal lobe epilepsy. Epilepsia 1994;35:721–7.
Sperling MR, O'Connor MJ. Auras and subclinical seizures: characteristics and prognostic significance. Ann Neurol 1990;28:320–8.
Staba RJ, Wilson CL, Bragin A, Fried I, Engel Jr J. Quantitative analysis of high-frequency oscillations (80–500 Hz) recorded in human epileptic hippocampus and entorhinal cortex. J Neurophysiol 2002;88:1743–52.
Staba RJ, Frighetto L, Behnke EJ, Mathern GW, Fields T, Bragin A, et al. Increased fast ripple to ripple ratios correlate with reduced hippocampal volumes and neuron loss in temporal lobe epilepsy patients. Epilepsia 2007;48:2130–8.
Tamraz JC, Comair YG. Atlas of regional anatomy of the brain using MRI: with functional correlations. Berlin Heidelberg: Springer-Verlag; 2000.
Thom M, Liagkouras I, Martinian L, Liu J, Catarino CB, Sisodiya SM. Variability of sclerosis along the longitudinal hippocampal axis in epilepsy: a post mortem study. Epilepsy Res 2012;102:45–59.
Van Paesschen W, King MD, Duncan JS, Connelly A. The amygdala and temporal lobe simple partial seizures: a prospective and quantitative MRI study. Epilepsia 2001;42:857–62.

Waldman ZJ, Shimamoto S, Song I, Orosz I, Bragin A, Fried I, et al. A method for the topographical identification and quantification of high frequency oscillations in intracranial electroencephalography recordings. Clin Neurophysiol 2018;129:308–18.
Wennberg R, Arruda F, Quesney LF, Olivier A. Preeminence of extrahippocampal structures in the generation of mesial temporal seizures: evidence from human depth electrode recordings. Epilepsia 2002;43:716–26.
Wilder BJ. The mirror focus and secondary epileptogenesis. Int Rev Neurobiol 2001;45:435–46.
Worrell GA, Gardner AB, Stead SM, Hu S, Goerss S, Cascino GJ, et al. High-frequency oscillations in human temporal lobe: simultaneous microwire and clinical macroelectrode recordings. Brain 2008;131:928–37.
Yilmazer-Hanke DM, Wolf HK, Schramm J, Elger CE, Wiestler OD, Blümcke I. Subregional pathology of the amygdala complex and entorhinal region in surgical specimens from patients with pharmacoresistant temporal lobe epilepsy. J Neuropathol Exp Neurol 2000;59:907–20.
Zelmann R, Zijlmans M, Jacobs J, Châtillon CE, Gotman J. Improving the identification of high frequency oscillations. Clin Neurophysiol 2009;120:1457–64.
Zelmann R, Mari F, Jacobs J, Zijlmans M, Dubeau F, Gotman J. A comparison between detectors of high frequency oscillations. Clin Neurophysiol 2012;123:106–16.